


RESEARCH ARTICLE

Open Access



Transcriptome-wide m⁶A profiling reveals mRNA post-transcriptional modification of boar sperm during cryopreservation

Ziyue Qin^{1,2†}, Wencan Wang^{1,2†}, Malik Ahsan Ali^{1,2,3}, Yihan Wang^{1,2}, Yan Zhang^{1,2}, Ming Zhang^{1,2}, Guangbin Zhou^{1,2}, Jian-dong Yang^{1,2} and Changjun Zeng^{1,2*} 

Abstract

Background: Cryopreservation induces transcriptomic and epigenetic modifications that strongly impairs sperm quality and function, and thus decrease reproductive performance. N⁶-methyladenosine (m⁶A) RNA methylation varies in response to stress and has been implicated in multiple important biological processes, including post-transcriptional fate of mRNA, metabolism, and apoptosis. This study aimed to explore whether cryopreservation induces m⁶A modification of mRNAs associated with sperm energy metabolism, cryoinjuries, and freezability.

Results: The mRNA and protein expression of m⁶A modification enzymes were significantly dysregulated in sperm after cryopreservation. Furthermore, m⁶A peaks were mainly enriched in coding regions and near stop codons with classical RRACH motifs. The mRNAs containing highly methylated m⁶A peaks (fts vs. fs) were significantly associated with metabolism and gene expression, while the genes with less methylated m⁶A peaks were primarily involved in processes regulating RNA metabolism and transcription. Furthermore, the joint analysis of DMMGs and differentially expressed genes indicated that both of these play a vital role in sperm energy metabolism and apoptosis.

Conclusions: Our study is the first to reveal the dynamic m⁶A modification of mRNAs in boar sperm during cryopreservation. These epigenetic modifications may affect mRNA expression and are closely related to sperm motility, apoptosis, and metabolism, which will provide novel insights into understanding of the cryoinjuries or freezability of boar sperm during cryopreservation.

Keywords: N⁶-methyladenosine (m⁶A), Boar sperm, Cryopreservation, MeRIP-seq

Background

Cryopreservation is a vital procedure with extensive applications for long-term semen storage, despite the associated risk for sperm cryoinjuries, including impaired motility, fertility, and apoptosis, due to oxidative stress

[1–4]. In commercial swine herds, only about 1 % of artificial insemination (AI) worldwide is practiced with post-thawed semen as it results in decreased conception rate and litter size [5–7]. Therefore, the study of molecular markers and underlying mechanisms related to cold shock and freeze tolerance is imperative to improve AI outcomes. Sperm epigenetic markers, such as DNA methylation, histone modification, and non-coding RNAs are associated with successful fertilization and healthier offspring [8, 9]. It is well documented that external chemicals, radiation, and stress can elicit remarkable epigenetic changes in boar sperm. Previously, we

* Correspondence: zengcj@sicau.edu.cn

[†]Ziyue Qin and Wencan Wang contributed equally to this work.

¹College of Animal Sciences and Technology, Sichuan Agricultural University, 611130 Chengdu, Sichuan, China

²Farm Animal Genetic Resources Exploration and Innovation Key Laboratory of Sichuan Province, Sichuan Agricultural University, 611130 Chengdu, Sichuan Province, China

Full list of author information is available at the end of the article



© The Author(s). 2021 **Open Access** This article is licensed under a Creative Commons Attribution 4.0 International License, which permits use, sharing, adaptation, distribution and reproduction in any medium or format, as long as you give appropriate credit to the original author(s) and the source, provide a link to the Creative Commons licence, and indicate if changes were made. The images or other third party material in this article are included in the article's Creative Commons licence, unless indicated otherwise in a credit line to the material. If material is not included in the article's Creative Commons licence and your intended use is not permitted by statutory regulation or exceeds the permitted use, you will need to obtain permission directly from the copyright holder. To view a copy of this licence, visit <http://creativecommons.org/licenses/by/4.0/>. The Creative Commons Public Domain Dedication waiver (<http://creativecommons.org/publicdomain/zero/1.0/>) applies to the data made available in this article, unless otherwise stated in a credit line to the data.

have detected dramatic changes in the expression of epigenetic-related genes, such as *Dnmt3a* and *Dnmt3b*, during boar sperm cryopreservation [10]. Likewise, the level of DNA methylation in horse sperm increased significantly after cryopreservation, and this may partially explain the low fertility of mares after insemination with frozen-thawed semen [11]. However, little is known about how RNA methylation modifications in sperm respond to external stimuli.

So far, over 100 chemical modifications on RNAs, especially on transfer RNA (tRNA) and ribosomal RNA (rRNA) have been discovered [12, 13]. N⁶-methyladenosine (m⁶A) is the most prevalent post-transcriptional modification of mRNA and is ubiquitous in various species, including mammals [14, 15], plants [16], fruit flies [17], yeast [18], and viruses [19]. The mammalian m⁶A methylation is catalyzed by several methyltransferases, including methyltransferase-like 3 (METTL3), methyltransferase-like 14 (METTL14), and Wilms' tumor 1-associating protein (WTAP). Conversely, Fat mass and obesity-associated protein (FTO) and alkB homolog 5 (ALKBH5) act as demethylases and remove the m⁶A modification from RNAs. YTHDF1/2/3, a class of specific m⁶A reader proteins, are responsible for the biological functions of m⁶A modification [20]. In addition, m⁶A modifications are an extremely important epigenetic modification that regulate post-transcriptional gene expression by regulating the splicing, stability, degradation, and translation of m⁶A modified mRNAs [21–23].

In mammals, increasing evidence supports the crucial biological functions of mRNA m⁶A methylation in sperm. Previous studies indicated that knock-out of m⁶A modification enzymes leads to lower sperm count, motility, and fertility in mouse [24, 25]. Tang et al. found that m⁶A modification controls the fate of mRNAs with a long 3'UTR by ALKBH5-dependent demethylation during spermatogenesis [26]. Further work showed that depletion of ALKBH5 facilitates the biogenesis of translatable circRNAs, whose translation initiation is mediated by YTHDF3-dependent recognition of start codon by m⁶A methylation [27]. Compared with normal sperm, the m⁶A content and *METTL3* expression in asthenospermic patients were significantly increased, suggesting that an abnormal increase of m⁶A modification in human sperm may greatly affect sperm motility and m⁶A modification enzymes (*METTL3*, *METTL14*, *FTO*, *ALKBH5*, *YTHDF2*) were implicated in modulating m⁶A contents in sperm RNA [28]. Landfors et al. identified two missense mutations of the FTO protein in human sperm, which led to functional defects in m⁶A demethylation and declining sperm quality [29].

Generally, the extent of m⁶A methylation, as well as the m⁶A-protein level, may reflect quality and fertilizing capacity of sperm during cryopreservation.

RNA-seq is a widely used technology for high-throughput analysis of transcriptomic profiles, and the study of the sperm transcriptomes is crucial for understanding its biology and role in fertility [30]. Multiple studies have used RNA-seq to evaluate differentially expressed transcripts in boar sperm and have demonstrated the involvement of multiple genes in regulating vital physiological functions [31, 32]. Moreover, these transcripts can be used as a reference for the identification of markers of sperm quality in pigs. In addition, methylated RNA immunoprecipitation sequencing (MeRIP-seq) is a common approach based on RNA-seq to profile and predict m⁶A modifications across the transcriptome. MeRIP-seq can be employed to detect m⁶A modifications at specific loci to provide insight into the regulatory mechanisms underlying environmental response [33]. In this study, fresh sperm (Fs) and frozen-thawed sperm (Fts) from boar were used for profiling the transcriptome-wide m⁶A methylation patterns by MeRIP-seq. In addition, we performed RNA-Seq and carried out a combined analysis of m⁶A methylation and mRNA levels. We found highly diverse m⁶A patterns between Fs and Fts, and speculate that study of m⁶A modification patterns may present an opportunity to deepen our understanding of the role of epigenetic modifications in regulating sperm function during cryopreservation.

Results

Cryopreservation of boar sperm altered mRNA and expression of m⁶A modification enzymes

Using RT-qPCR and western blot (WB), we assessed differences in mRNA and protein levels of five major enzymes responsible for m⁶A modification between Fs and Fts, including *METTL3*, *METTL14*, *FTO*, *ALKBH5* and *YTHDF2*. The mRNA expression levels of *METTL3*, *METTL14*, *ALKBH5*, and *YTHDF2* were significantly decreased in the Fts group, whereas the *FTO* gene showed significantly increased expression ($P < 0.05$) (Fig. 1A). The protein levels of *METTL3*, *METTL14*, and *FTO* were downregulated in response to cryopreservation ($P < 0.01$), whereas *ALKBH5* and *YTHDF2* were upregulated in the Fts group ($P < 0.01$, Fig. 1B C). Therefore, we speculate that cryopreservation induces m⁶A methylation by regulating the mRNA and protein levels of five major enzymes responsible for m⁶A modifications.

Overview of transcriptome-wide m⁶A methylation of boar Fs and Fts

An average of more than 78,000,000 clean reads were obtained from 12 libraries in Fs IP and Fts IP groups by MeRIP-Seq (Table S1). Furthermore, the mapping ratio

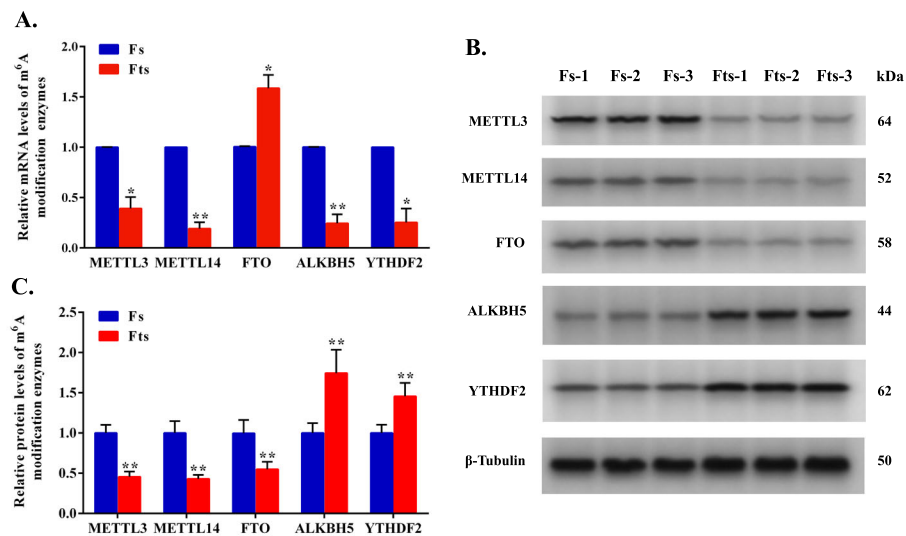


Fig. 1 m⁶A modification enzymes of boar sperm are dysregulated after cryopreservation. **A** Relative mRNA expression levels of m⁶A modification enzymes in Fs and Fts assessed by RT-qPCR. **B** WB bands illustrating the protein levels of m⁶A modification enzymes and β-tubulin in Fs and Fts. **C** Histogram showing the relative protein levels of m⁶A modification enzymes in Fs and Fts. Values were normalized using β-tubulin protein as an internal reference. Fs, fresh sperm; Fts, frozen-thawed sperm. “**P* < 0.05, ***P* < 0.01”

of clean reads in both Fs IP and Fts IP groups exceeded 75.09 % when matched to the reference genome (UCSC susScr11) (Table S1).

A total of 3,647 and 4,033 m⁶A peaks were identified in Fs and Fts, respectively. Of these, 1,048 peaks (~ 16 % of all peaks in both Fs and Fts) were common to both Fs and Fts samples (Fig. 2A). Compared with Fs, 1,613 significantly hyper-methylated peaks among 1,442 mRNAs and 315 significantly hypo-methylated peaks within 312 mRNAs (|fold change| ≥ 2 and *P* < 0.00001) in Fts were identified (Fig. 2B, Table S2-1, S2-2). The top 10 significantly increased and decreased m⁶A peaks in Fts are listed in Table S3 and Table S4, respectively.

To determine the conserved RRACH (R = purine, A = m⁶A and H = non-guanine base) motif in all identified m⁶A peaks, the top 2000 m⁶A-containing peaks from all sperm samples were analyzed. Out of these, five motif consensus sequences were listed by enrichment, consistent with former studies, reinforcing the authenticity of the data (Fig. 2C). In addition, metagene profile analysis indicated that m⁶A peaks were preferentially located at coding regions (CDS), at start codons, and near stop codons in both Fs and Fts groups; Fts had higher proportion of m⁶A peak enrichment in CDS than Fs (Fig. 2D and E). Generally, about 80 and 70 % of m⁶A-containing genes had only one m⁶A peak in Fs and Fts, respectively. The number of transcripts containing two or more peaks in Fts was greater than in Fs (Fig. 2F).

Distribution of differentially methylated m⁶A sites (DMMSs)

All differentially methylated m⁶A sites (DMMSs) within mRNAs were mapped to chromosomes to evaluate their distribution profiles (Fig. 3A). The top five chromosomes with the highest relative densities of DMMS normalized to chromosome length, in decreasing order, were 12, 3, 14, 2 and 7 (Fig. 3B). By using Integrative Genomics Viewer (IGV, v2.8.2) software, we displayed two representative DMMSs selected from MeRIP-seq, *SORD* (hypermethylated peak) and *NAGK* (hypomethylated peak), which showed altered m⁶A intensity (Fig. 3C). Further, we conducted an independent methylated RNA immunoprecipitation-qPCR (MeRIP-qPCR) experiment to detect total mRNA m⁶A levels of ten randomly selected genes with DMMSs. Notably, six hypermethylated genes, *FOXO3*, *NADK2*, *ACLY*, *HIF1A*, *SLC9A3R1*, and *PKM*, and one hypomethylated gene, *FASN*, were reported to be involved in regulation of sperm quality. All of these genes have significantly altered total mRNA m⁶A levels as measured by MeRIP-qPCR (Fig. 3D). Among these, the m⁶A levels of nine genes were consistent with MeRIP-seq data; conversely, the total m⁶A level of *FASN* was reduced in Fts by MeRIP-qPCR but showed an increase in the MeRIP-seq data. These results confirm the accuracy of our sequencing data.

GO and KEGG pathway analysis of genes containing significantly altered m⁶A peaks (DMMGs)

In order to explore the physiological functions of m⁶A methylation in Fts, the genes containing significantly

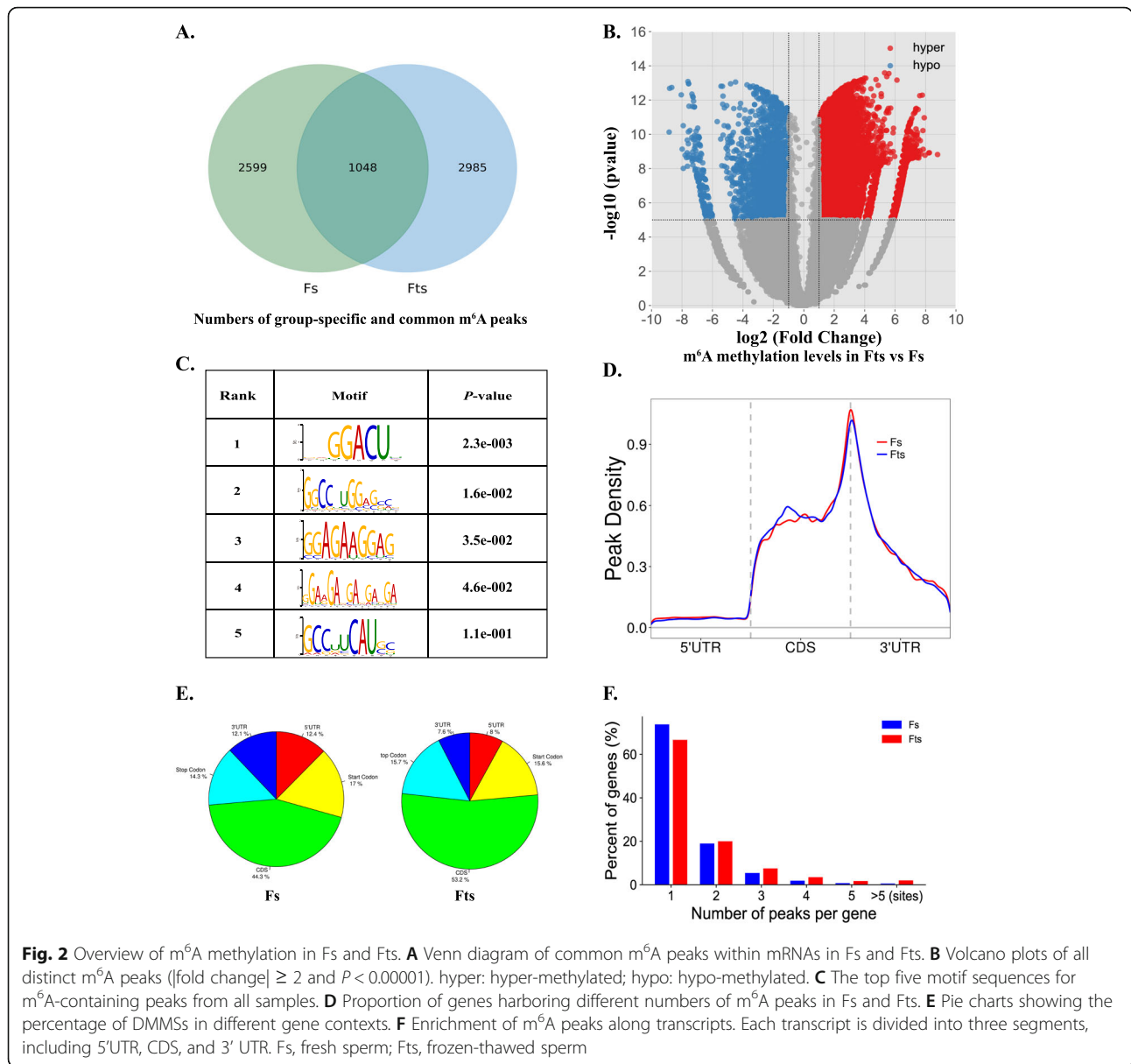


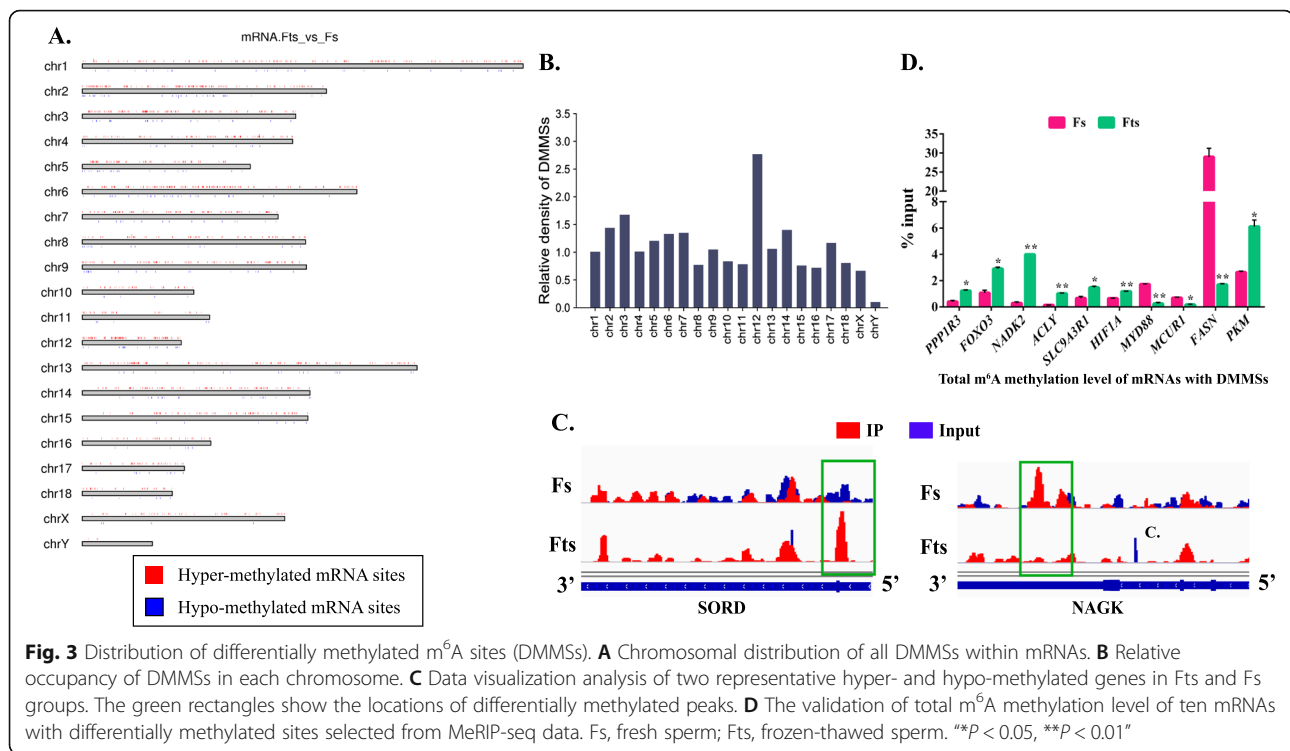
Fig. 2 Overview of m⁶A methylation in Fs and Fts. **A** Venn diagram of common m⁶A peaks within mRNAs in Fs and Fts. **B** Volcano plots of all distinct m⁶A peaks (|fold change| ≥ 2 and P < 0.00001). hyper: hyper-methylated; hypo: hypo-methylated. **C** The top five motif sequences for m⁶A-containing peaks from all samples. **D** Proportion of genes harboring different numbers of m⁶A peaks showing the percentage of DMMSs in different gene contexts. **E** Enrichment of m⁶A peaks along transcripts. Each transcript is divided into three segments, including 5'UTR, CDS, and 3' UTR. Fs, fresh sperm; Fts, frozen-thawed sperm

altered m⁶A peaks (differentially methylated m⁶A genes, DMMGs) were subjected to GO and KEGG pathway analysis. GO analysis (biological process, BP; cellular component, CC; molecular function, MF; Table S5-1, S5-2) of the hyper- and hypo-methylated genes in Fts showed that hyper-methylated genes were significantly (P < 0.05) involved in metabolism, including in macromolecule metabolic process and organic substance metabolic process, gene expression, and transcription (ontology: BP). Furthermore, these genes also play a part in cell and intracellular organelles (ontology: CC) and protein binding (ontology: MF, Fig. 4A). Hypo-methylated genes in Fts were significantly enriched in transcription from RNA polymerase II promoter, regulation of RNA metabolic process, regulation of

transcription, and DNA-templating (ontology: BP), external side of plasma membrane (ontology: CC), and transcriptional regulatory region DNA binding and enzyme binding (ontology: MF, Fig. 4B). Moreover, KEGG pathway analysis revealed that hyper- and hypo-methylated m⁶A sites representing genes in Fts were enriched in mTOR, AMPK, MAPK, and TGF-beta signaling pathways (Fig. 4C, D, Table S6-1, S6-2).

Joint analysis of DMMGs and differentially expressed genes (DEGs)

Given the indispensable function of RNA m⁶A modifications in regulating gene expression, transcriptome profiles of altered genes in Fts were determined by RNA-seq. Scatter plots showed the presence of 295



significantly up-regulated genes and 2,071 significantly down-regulated genes ($|\text{fold change}| \geq 2$, $P < 0.05$) between Fs and Fts (Fig. 5A, Table S7-1, S7-2). All genes were divided into four groups based on joint analysis of DMMGs and DEGs, including 13 hyper-methylated & up-regulated genes (hyper-up), 19 hypo-methylated & down-regulated genes (hypo-down), 149 hyper-methylated & down-regulated genes (hyper-down), and 3 hypo-methylated & up-regulated genes (hypo-up) (Fig. 5B). Notably, 88.7% (149/168) of the down-regulated mRNAs contained hyper-methylated m⁶A peaks. GO and KEGG analysis revealed that DEGs containing hyper- and hypo-methylated m⁶A peaks were significantly enriched in many important biological processes and pathways, such as sperm capacitation, calcium-mediated signaling, sperm motility, and apoptosis (Fig. 5C, D, Table S8). Nine differentially methylated DEGs between Fs and Fts, associated with sperm quality and function, including regulation of sperm motility and capacitation, are listed in Table 1.

Discussion

The process of freezing-thawing induces dramatic changes in sperm, including osmolarity, volume, and oxidative stress [43, 44]. These rapid transitions could affect cell membrane fluidity, plasma membrane integrity, and DNA structure [45, 46]. In addition, dysregulation of redox homeostasis [47] and mitochondrial activity [48], and expression of cryoinjury-related genes

[49, 50] could eventually impair morphology, motility, and metabolism of frozen-thawed sperm [51]. Recent studies indicated that cryopreservation as an environmental stimulus alters transcript, non-coding RNA (miRNAs, lncRNAs etc.), and protein levels. These altered transcripts, non-coding RNA, and proteins were demonstrated to be associated with post-thawed sperm quality, such as motility, survival, fertility, and early embryonic development [52]. Moreover, the process of freezing and thawing also induces an alteration of sperm epigenetics [10, 11]. However, transcriptome-wide epigenetic modifications in sperm have not been reported. Previous studies demonstrated that m⁶A methylation was significantly associated with cellular response to environmental stimuli, such as endocrine-disrupting chemicals [53], oxidative stress [54], and inflammation [55]. In this study, we first found that the methyltransferases METTL3 and METTL14 were down-regulated in frozen-thawed sperm. Conversely, the protein levels of FTO, ALKBH5, and YTHDF2 were inconsistent with their mRNA levels. Previous studies demonstrated that freezing-thawing treatment affects mRNA-protein interactions and makes mRNA more susceptible to degradation [56]. Moreover, the decrease of some transcripts might also result from an increase in translation for more protein synthesis [57]. Oxidative stress could induce elevated m⁶A levels and up-regulate the expression of FTO without affecting protein levels. Thus, cryoprotectant might exert a protective effect against oxidative

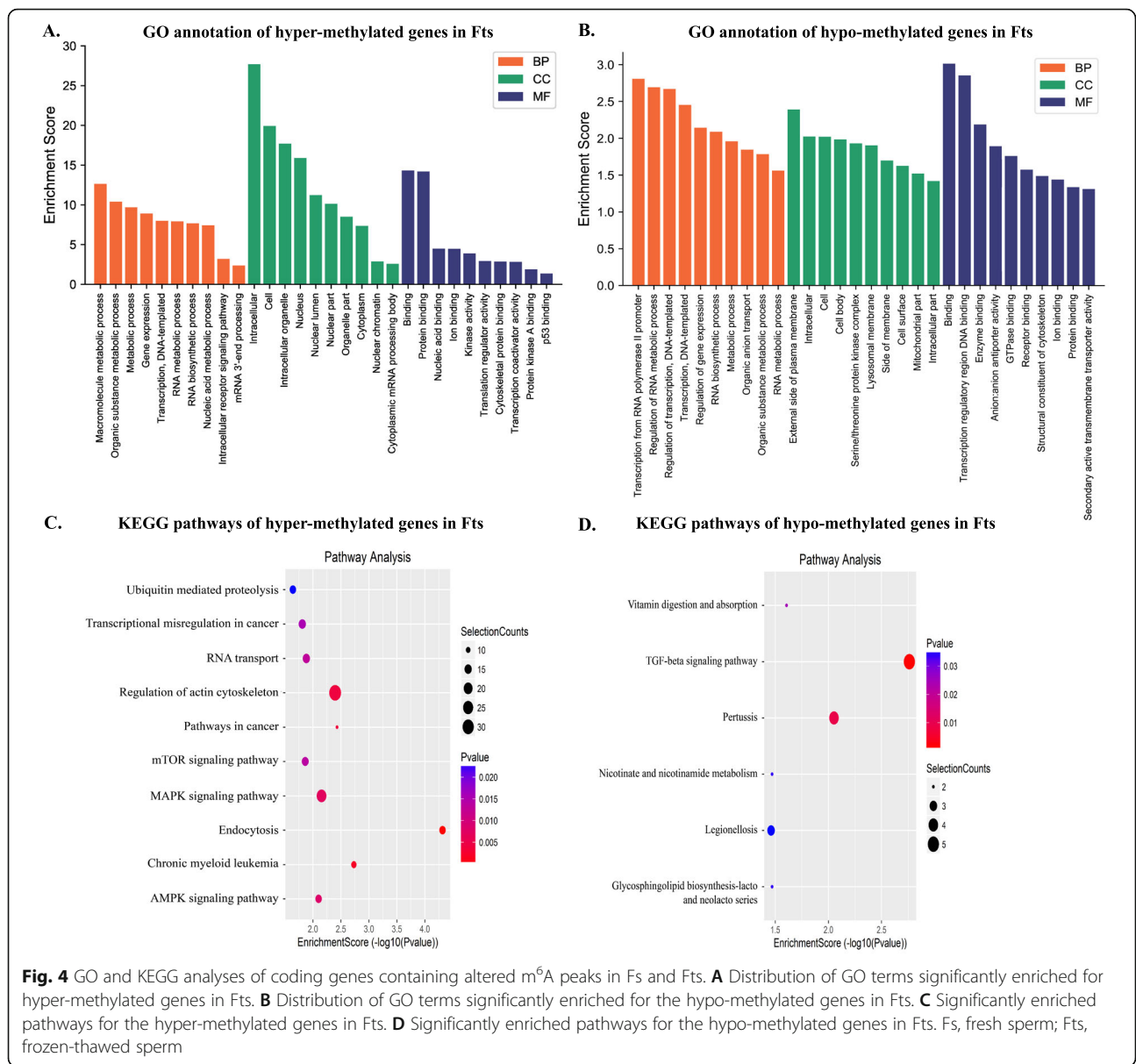


Fig. 4 GO and KEGG analyses of coding genes containing altered m⁶A peaks in Fs and FtS. **A** Distribution of GO terms significantly enriched for hyper-methylated genes in FtS. **B** Distribution of GO terms significantly enriched for the hypo-methylated genes in FtS. **C** Significantly enriched pathways for the hyper-methylated genes in FtS. **D** Significantly enriched pathways for the hypo-methylated genes in FtS. Fs, fresh sperm; FtS, frozen-thawed sperm

stress by inhibiting of the expression of FTO in sperm [58]. mRNA levels of key m⁶A modification enzymes, including METTL3, METTL14, FTO, and YTHDF2, are highly correlated with the proportion of m⁶A modifications of total mRNA [59]. Germ cell-specific inactivation of METTL3 and METTL14 causes loss of m⁶A modifications [24]. Overexpression of ALKBH5 can suppress the expression of m⁶A-modified mRNA [60]. Additionally, the m⁶A modification reader YTHDF2 shows identical binding to all m⁶A sites in mRNAs and mediates the degradation of m⁶A-mRNAs [61, 62]. These findings suggest that cryopreservation may affect the methylation level and stability of m⁶A-modified mRNA, which reflects the metabolic status of a cell under environment stress. In the present study, we investigated the

importance of m⁶A methylation in sperm by using MeRIP-seq to determine the mRNA m⁶A profiles of Fs and FtS.

We discovered unique patterns of m⁶A modifications in mRNA from Fs and FtS. The motifs of m⁶A modification sites in sperm mRNA were revealed by enrichment analysis, which showed that the RRACH consensus sequences were consistent with other studies in various species [14, 63, 64]. Further, we found that m⁶A peaks were especially enriched in CDS, at start codons, and near stop codons, which is consistent with prior work in human and mice [14, 65]. Moreover, m⁶A methylation patterns in sperm are the same as in other tissues of the pig, such as fat and muscle [66], which further confirms that features of

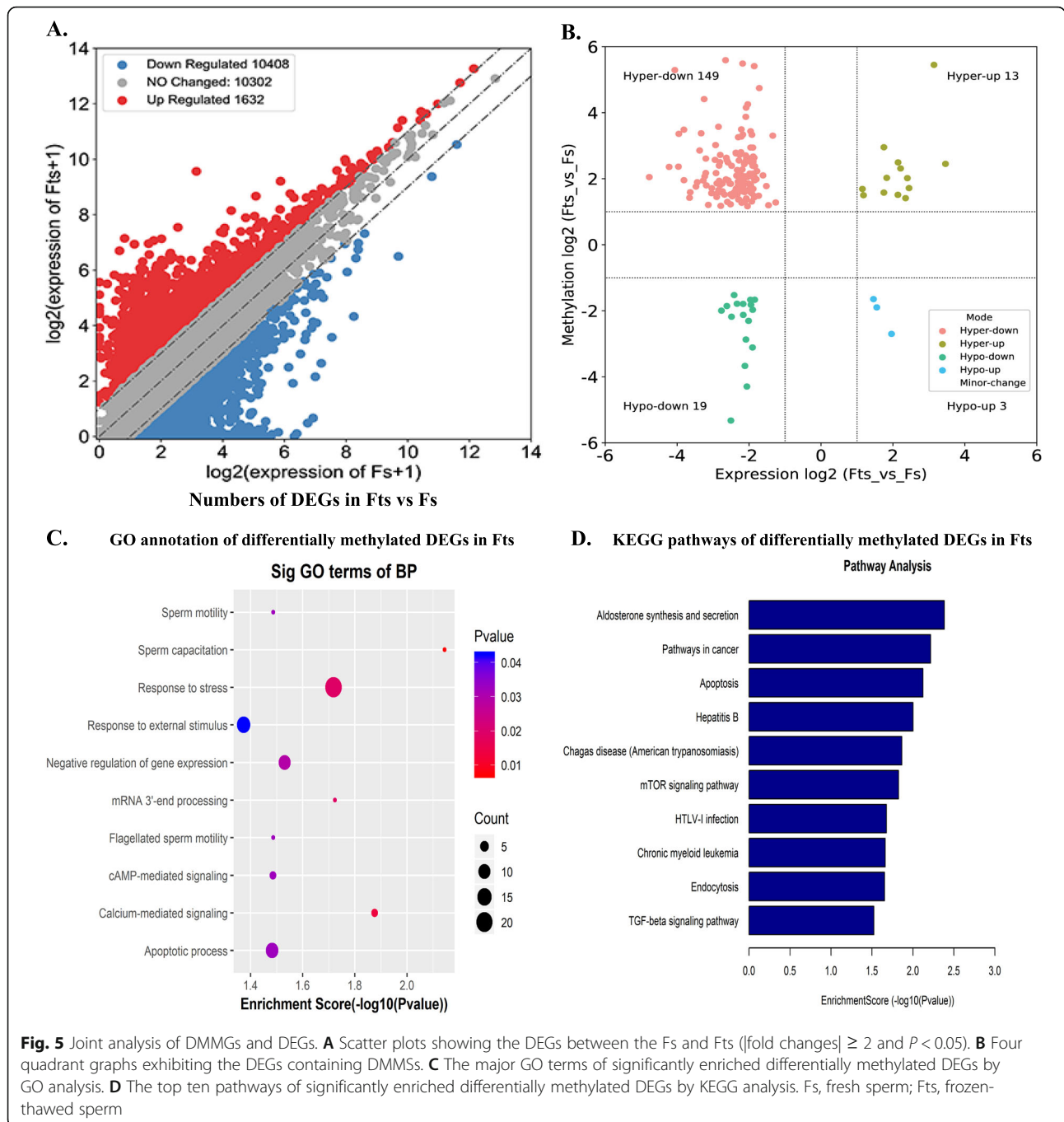


Fig. 5 Joint analysis of DMMGs and DEGs. **A** Scatter plots showing the DEGs between the Fs and Fts ($|\text{fold changes}| \geq 2$ and $P < 0.05$). **B** Four quadrant graphs exhibiting the DEGs containing DMMGs. **C** The major GO terms of significantly enriched differentially methylated DEGs by GO analysis. **D** The top ten pathways of significantly enriched differentially methylated DEGs by KEGG analysis. Fs, fresh sperm; Fts, frozen-thawed sperm

RNA m⁶A methylation are conserved in pig. We identified numerous m⁶A peaks that varied widely among individual transcripts, and most of them harbored only one or two m⁶A peaks, which was consistent with previous studies in humans [67] and chickens [68]. Analysis at the whole chromosome level showed that mRNAs containing altered m⁶A peaks were transcribed from all chromosomes, especially autosomes [67, 69], indicating that m⁶A modification patterns in Fts are widely changed and may involve many

pathways that influence the function of sperm. Furthermore, the total m⁶A level of nine transcripts (*PPP1R3*, *FOXO3*, *NADK2*, *ACLY*, *SLC9A3R1*, *HIF1A*, *MYD88*, *MCUR1*, and *PKM*) were evaluated using MeRIP-qPCR and found to be consistent with the MeRIP-seq results. The findings suggest that transcript identification and estimates of expression were highly reliable.

It has been demonstrated that a variety of signaling pathways and regulatory mechanisms participate in normal sperm function. Herein, GO and KEGG pathway

Table 1 Functions of the differentially expressed and methylated DEGs between Fs and Fts during cryopreservation

Gene symbol	Regulation (Fts vs. Fs)						Description
	Methylation	Fold Change	p_value	mRNA expression	Fold Change	p_value	
<i>ACLY</i>	Up	2.8	5.18E-06	Down	-inf	2.72e-02	Regulation of the ram sperm energy metabolism and ATP supplement [34, 35]
<i>PDE4A</i>	Up	2.8	4.67E-06	Up	2.3	3.14e-02	Regulation of bovine sperm motility [36]
<i>NFATC3</i>	Up	11.3	3.20E-06	Down	-inf	7.20e-03	Differentially represented between fresh- and frozen-sperm in boar [31]
<i>BCL2L1</i>	Up	3.1	8.07E-06	Down	-inf	2.80e-03	Cell apoptosis protecting [37]
<i>CARD6</i>	Up	2.9	4.07E-06	Down	-inf	5.00e-05	Regulation of apoptosis [38]
<i>PIK3R1</i>	Up	3.2	2.56E-06	Down	-inf	5.00e-05	Involved in actin polymerization during bovine sperm capacitation [39]
<i>NCALD</i>	Up	2.3	1.13E-06	Down	-inf	5.00e-05	Regulation of Calcium-modulated transduction in human and bovine sperm [40]
<i>SOX9</i>	Up	11.0	8.73E-07	Down	-inf	5.00e-05	Regulate male fertility in mice [41]
<i>PLCB1</i>	Up	7.7	5.65E-06	Down	-inf	9.50e-04	Essential for acrosome reaction and fertilization in mouse sperm [42]

Note: -inf means negative infinity

analyses were performed to deduce potential functions of DMMGs. GO analysis revealed that coding genes with altered m⁶A peaks were mainly involved in biological processes such as metabolism, gene expression, and regulation of RNA metabolism. Cryopreservation impairs numerous proteins implicated in mitochondrial tricarboxylic acid (TCA) cycle and oxidative phosphorylation, which contribute to proper metabolism and oxidoreductase activity in sperm [70]. Cryodamage is also involved in the degradation of certain mRNAs; therefore, it could impair the function of relevant proteins [50]. Natural modifications of cellular RNA enable the orderly metabolism and function of diverse RNA species, thereby affecting gene expression [71]. Recent studies have suggested that environmental perturbations could induce epigenetic changes in the testis. After exposure to environmental toxins, genes with differentially methylated DNA regions or differentially expressed mRNA in Sertoli cells of F3 generation rats were enriched in categories including metabolism, transcription, and cytoskeleton [72]. Therefore, m⁶A methylation may mediate the regulation of sperm RNA levels and metabolism during cryopreservation. KEGG analysis revealed that DMMGs were significantly enriched in the ubiquitin mediated proteolysis, AMPK, mTOR, and MAPK signaling pathways, which are known to control stress response, apoptosis, and capacitation in sperm [73, 74]. Ubiquitin acts as a molecular marker and tags proteins for degradation by the proteasome. High sperm surface ubiquitination is coupled with lower developmental competence of pig embryos [75]. Cryopreservation induced a significant decrease in the percentage of ubiquitinated boar sperm, and the ability of frozen-thawed sperm to capacitate and of the acrosome to react

were both influenced by ubiquitination [76]. AMPK is a key kinase involved in regulating the cellular redox state by switching metabolic pathways under stressful conditions. Zhu et al. reported that resveratrol is beneficial for improving the quality of post-thaw boar sperm by activating the AMPK pathway to reduce sperm apoptosis [3]. The PI3K/AKT/mTOR signaling pathway is involved in the regulation of sperm autophagy and mTOR is considered a central integrator of several signals, allowing it to regulate metabolism and redox balance [77]. Furthermore, the process of freezing and thawing can activate p53 via the p38/MAPK pathway and subsequently cause apoptosis in sperm [78]. Similar KEGG pathways, including MAPK, TGF-beta, and ubiquitin-mediated proteolysis signaling pathways, which are directly linked with sperm quality, contain miRNAs that were differentially expressed in sperm exposed to fluoride [79]. In addition, a series of DMMGs were found to participate in stress response, apoptosis, substrate metabolism, and sperm motility. Sirtuin 1 (*SIRT1*), a histone deacetylase, was found to be involved in regulating transcription, energy metabolism, and oxidative stress and to contribute to sperm abnormalities in infertile men [80–82]. Evidence indicates that increased expression of *SIRT1* could suppress spermatogonial cell apoptosis, and DNA hypermethylation of *SIRT1* promotes down-regulation of *SIRT1* expression [83, 84]. Defects in Parkinsonism-associated protein 7 (*Park7*, also known as *DJ-1*), an oxidative stress response product, have been widely reported to be correlated with male infertility [85–87]. Recently, *Park7* was observed as a target gene for the mitochondria-related miRNA miR-4485-3p which may link mitochondrial dysfunction and male asthenozoospermia [88]. Kinesins (*KIFs*) are a superfamily of motor proteins

and have been reported to play a role in sperm motility and apoptosis [89–92]. In our data, some differentially methylated *KIF* genes were also detected, including *KIF1B*, *KIF5A*, *KIF5B*, and *KIF15*. Interestingly, both hyper- and hypo-methylated peaks on the mRNA of *KIF5B* (2.8- and 11.6-fold change, respectively) were detected. Similarly, *NDUFS1*, an oxidative phosphorylation marker, whose mRNA methylation increased 3.2-fold after cryopreservation in our study, was detected at low levels in semen collected from patients with testicular cancer and at high levels in the sperm of infertile men [93, 94]. Sorbitol dehydrogenase (*SORD*) converts sorbitol to fructose, which can be further metabolized via the glycolytic pathway to yield ATP [95]. This reproduction-related gene is also involved in the maturation and capacitation of sperm [96]. Moreover, N-acetyl glucosamine kinase (*NAGK*) was predicted to significantly affect ATP production and regulate metabolism in asthenozoospermia [97]. As shown in Fig. 3C, *SORD* and *NAGK* mRNA were hyper-methylated and hypo-methylated in the Fts group, respectively. In the present study, all of the above-mentioned genes in sperm showed different m⁶A methylation after cryopreservation, but their expression levels did not change significantly. Thus, we propose that m⁶A methylation may affect other conditions related to these genes to regulate the viability, motility, and energy metabolism of boar sperm, which should be investigated in future studies.

Our previous data from transcriptome sequencing of fresh and frozen-thawed boar sperm revealed that DEGs in frozen sperm are enriched in many important biological processes and pathways, such as sperm motility, metabolism, and apoptosis [98], which is in accordance with our present study of differentially methylated DEGs showing enrichment in these pathways (Table 1). Among these genes, ATP citrate lyase (*ACLY*), a vital gene involved in the TCA cycle whose mRNA was hyper-methylated and down-regulated in the Fts group, has been implicated in male infertility [99]. Further, previous studies also demonstrated that *ACLY* can regulate sperm energy metabolism and ATP production [34, 35]. Phosphodiesterase 4 A (*PDE4A*), whose mRNA was found to be hyper-methylated and up-regulated after cryopreservation in our study, regulates the motility of bovine sperm [36]. In addition, studies have shown that *PDE4A* can modulate sperm chemotaxis by controlling the level of cAMP during fertilization [100, 101]. The mRNA of nuclear factor of activated T cells 3 (*NFATC3*), a potential marker for predicting the freezability of boar sperm [31], was found to be hyper-methylated and down-regulated in the Fts group. Moreover, BCL2-like 1 (*BCL2L1*), an apoptosis-related gene was reported to prevent apoptosis by inhibiting the release of

cytochrome c from mitochondria [37]. Claudin domain containing 1 (*CLDN1*) and Caspase recruitment domain family member 6 (*CARD6*) were found to regulate the apoptosis in breast cancer and non-alcoholic fatty liver disease, respectively [38, 102]. In our combined analysis, we found simultaneous changes in the mRNA m⁶A methylation and expression levels of these genes in the Fts group. Numerous studies have substantiated that m⁶A modification in mRNAs could control RNA translation and transcript fate [103, 104]. The impacts of m⁶A on the transcriptome are attributed to the cross-talk among m⁶A readers, writer-complex components, as well as potential erasers, the significance of which remains to be elucidated. Liu et al. reported that knockout of METTL3 or YTHDC1 could enhance chromatin accessibility and activate transcription in an m⁶A-dependent manner [105]. Additionally, knock-down of the m⁶A reader HNRNPA2B1 in human esophageal epithelial cells decreased mRNA expression of *ACLY* [106], and depletion of FTO leads to increased m⁶A levels in total RNA and reduces protein levels of *ACLY* in HepG2 cells [107]. These results indicate that m⁶A modification can modulate *ACLY* expression; therefore, it will be worthwhile to further explore the correlation between *ACLY* activity and m⁶A levels, as well as the exact mechanism underlying *ACLY* regulatory effects on sperm.

Conclusions

Our study, for the first time, comprehensively characterized transcriptome-wide m⁶A methylation profiles in boar spermatozoa. We revealed general characteristics, topological patterns, and differences of m⁶A modification and methylation profiles between fresh and frozen-thawed boar sperm. Compared to controls, the number and enrichment levels of m⁶A modified sites on transcripts, as well as the percentage of m⁶A peaks distributed among coding regions, were increased in frozen-thawed sperm. Moreover, joint analysis of MeRIP-seq and RNA-seq data indicated that DEGs containing DMMSs participate in sperm metabolism, apoptosis, and motility. The process of cryopreservation dysregulates m⁶A modification of mRNA, which may be responsible for cryoinjuries or freezability of boar sperm. Together, our work provides new evidence that cryopreservation induces epigenetic modifications of sperm. However, further studies should be conducted to better elucidate the correlation between m⁶A mRNA modification and sperm function.

Methods

Animal ethics statement

All procedures for animal treatments were reviewed and written approved by the Institutional Animal Care and

Use Committee in the College of Animal Science and Technology, Sichuan Agricultural University, Sichuan, China, under permit No. DKYB20081003.

Semen collection and cryopreservation

Fresh ejaculates with sperm-rich fractions were collected from three healthy, mature, and fertile Duroc boars, provided by Pengzhou Jinzhu Agricultural Development Co., Ltd (Pengzhou, Sichuan, China), using the gloved-hand technique during the autumn-winter period. All ejaculates with morphologically normal, more than 0.8 sperm motility and $1 \times 10^8 \text{ mL}^{-1}$ of sperm concentration were used. The basic extender used for sperm dilution was Beltsville thawing solution (BTS). The fresh ejaculates of each boar were equally divided into two parts and one was immediately exposed to liquid nitrogen ($-196 \text{ }^\circ\text{C}$) and then stored at $-80 \text{ }^\circ\text{C}$ for RNA extraction (Fs). Another part (Fts) was cryopreserved according to our previously described procedure [108]. Briefly, all semen samples were diluted and slowly cooled to $17 \text{ }^\circ\text{C}$ for 2 h, then centrifuged for 5 min at 1800 rpm. The sperm pellets were diluted with lactose-egg yolk (LEY) extender containing 11 % β -lactose (w/v) and 20 % hen's egg yolk (v/v) and slowly cooled to $4 \text{ }^\circ\text{C}$ for 4 h. Then, the semen samples were further diluted (2:1) with a second freezing extender (LEY supplemented with 6 % glycerol) and equilibrated at $4 \text{ }^\circ\text{C}$ for 30 min. Subsequently, the semen was loaded in previously labeled 0.2 mL straws (FHK, Tokyo, Japan) and equilibrated at approximately $-130 \text{ }^\circ\text{C}$ above liquid nitrogen vapor for 15 min, then the straws were plunged in liquid nitrogen ($-196 \text{ }^\circ\text{C}$) until use.

Total RNA extraction, cDNA synthesis and RT-qPCR

Before total RNA extraction, seminal plasma was removed by centrifuged for 5 min at 4000 rpm and washed with phosphate buffer solution (PBS) for three times. To eliminate somatic cell contamination, sperm pellet was treated with 0.5 % Triton X-100 (Coolaber, Beijing, China) [109]. Then, Total RNA from boar sperm was extracted with Trizol LS Reagent (Invitrogen Corporation, Carlsbad, CA, USA) according to the manufacturer's instructions. Furthermore, the concentration and purity of sperm RNA were determined by a Nanodrop (Thermo Fisher Scientific, Wilmington, DE, USA), while Agilent 2100 Bioanalyzer (Agilent Technologies, Santa Clara, CA, USA) was used to measure the RNA integrity. The SYBR Premix Ex Taq II Reagent Kit (Takara Biotech, Dalian, China) was used for RT-qPCR on the CFX 96 Real-Time PCR Detection System (Bio-Rad, Hercules, CA, USA). Briefly, 5 μL SYBR Green I Premix, 0.5 μL each of forward and reverse primers, 1 μL of cDNA, and sufficient RNase-free water were mixed to reach a total

volume of 10 μL . Then, the mixture was subjected to thermal cycling as follows: an initial denaturation step at $95 \text{ }^\circ\text{C}$ for 3 min, 40 cycles of amplification at $95 \text{ }^\circ\text{C}$ for 5 s, and primer-specific annealing temperatures were applied for 30 s. Relative expression levels were determined using the $2^{-\Delta\Delta\text{CT}}$ method [110]. According to counterparts in GenBank, all the primers were designed using NCBI Primer-Blast search (Table S9). The housekeeping gene, *GAPDH*, was used as the reference to evaluate the relative expression level of mRNAs [111].

Western blot analysis

Western blot of METTL3, METTL14, FTO, ALKBH5 and YTHDF2 was performed according to previous report [109] with some modifications. Briefly, after seminal plasma was removed, sperm pellets were re-suspended in a RIPA buffer (containing 1 % phenylmethylsulfonyl fluoride), placed on ice for 30 min and then centrifuged at 12,000 rpm, $4 \text{ }^\circ\text{C}$, for 5 min. The concentration of total protein was measured with a bicinchoninic acid (BCA) kit (Solarbio, Beijing, China) according to the manufacturer's protocol. The protein was separated by 12 % SDS-PAGE and electrophoretically transferred to PVDF membrane (Beyotime, Shanghai, China). Non-specific binding sites of protein were blocked in QuickBlock Western Buffer (Beyotime, Shanghai, China) for 1 h at room temperature and then incubated with primary antibodies [Anti-METTL3 (ab195352, Abcam), Anti-METTL14 (PA5-43606, Thermo Fisher), Anti-FTO (ab94482, Abcam), Anti-ALKBH5 (ab195377, Abcam), Anti-YTHDF2 (24744-1-AP, Proteintech), and anti- β -tubulin (ab21058, Abcam)] diluted in 5 % BSA in TBST (METTL3: 1:1000, METTL14: 1 $\mu\text{g}/\text{ml}$, FTO: 1 $\mu\text{g}/\text{ml}$, ALKBH5: 1:1000, YTHDF2: 1:5000, and β -tubulin 1:1000) overnight at $4 \text{ }^\circ\text{C}$ followed by incubation with HRP-conjugated secondary antibodies [goat anti-Rabbit IgG H&L (ab6721, Abcam), 1:10,000 dilution]. After washing the membrane with TBST (Beyotime, Shanghai, China), enhanced chemiluminescence detection was performed by using Immuno-Star™ Western™ Chemiluminescence Kit (BIO-RAD, Hercules, CA, USA) according to the manufacturer's protocol. The development of PVDF membrane were performed using ChemiScope 6000 Exp (CLiNX, Shanghai, China). Subsequently, band intensities were analyzed using a Gel-Pro Analyzer (Media Cybernetics, Bethesda, MD, USA). β -tubulin was used as the reference protein.

High-throughput m⁶A and RNA sequencing with data analysis

High-throughput m⁶A services were provided by Cloudseq Biotech Inc. (Cloudseq, Shanghai, China).

Briefly, total RNA was extracted using Trizol LS Reagent (Invitrogen Corporation, Carlsbad, CA, USA) following the manufacturer's instructions. The RiboZero rRNA Removal Kit (Illumina, Inc., San Diego, CA, USA) was used to reduce the ribosomal RNA content. Then, the RNA was chemically fragmented into fragments about 100 nucleotides in length using fragmentation buffer (Illumina, Inc., CA, USA). RNA fragments were incubated with anti-m⁶A polyclonal antibody (Synaptic Systems, Göttingen, Germany) in immunoprecipitation (IP) buffer for 2 h at 4°C. The mixture was then immunoprecipitated by incubation with protein-A beads (Thermo Fisher Scientific, Waltham, MA, USA) for 2 h at 4°C. Then, bound RNA was eluted from the beads with N⁶-methyladenosine (BERRY & ASSOCIATES, Ann Arbor, MI, USA) in IP buffer and then extracted with Trizol Reagent. The NEBNext[®] Ultra II Directional RNA Library Prep kit (New England Biolabs, Ipswich, MA, USA) was used to construct RNA sequence libraries for the non-immunoprecipitated input RNA samples (mRNA-seq) and immunoprecipitated IP RNA samples (MeRIP-seq). Library quality control was performed using the BioAnalyzer 2100 (Agilent, Santa Clara, CA, USA) and high-throughput sequencing was carried out in 150-bp double-end mode on an Illumina HiSeq 4000 sequencer (Illumina, Inc., San Diego, CA, USA). Image analysis, base recognition, quality control and original reads (Raw Data) were generated with the Illumina HiSeq 4000 sequencer. First, quality control was performed by Q30, which was followed by trimming of the 3' adaptors and removal of low-quality reads using cutadapt software (v1.9.3) [112]. Second, the clean reads of all samples were matched to the reference genome (UCSCusScr11, <http://hgdownload.soe.ucsc.edu/goldenPath/susScr11/bigZips/susScr11.fa.gz>) using Hisat2 software (v2.0.4) [113]. Third, the Model-based Analysis of ChIP-Seq (MACS) software [114] was used to identify the methylated genes in each sample, and non-immunoprecipitated input RNA was used as a correction for MACS peak calling. Differentially methylated sites with a |fold change| ≥ 2 and $P < 0.00001$ were identified with the diffReps software [115], and a proprietary program was used to screen the peaks on the mRNA for corresponding annotation. Identified m⁶A peaks were subjected to motif enrichment analysis using STREME software (v5.3.0) [116]. For RNA sequencing, raw counts of each feature were harvested by HTseq (v0.9.1) [117], and differentially expressed genes were identified using EdgeR software (v3.16.5) [118] with a |fold change| ≥ 2 and $P < 0.05$. GO analysis and KEGG pathway enrichment analysis were performed on the differentially methylated protein coding genes using

the GO (www.geneontology.org) and KEGG (www.genome.jp/kegg) databases.

MeRIP-qPCR

To validate MeRIP-seq results, the Magna MeRIP m⁶A kit (Millipore, Billerica, MA, USA) was used according to the manufacturer's instructions. Briefly, poly(A) RNA was first purified from 50 µg of total RNA using the Dynabeads[™] mRNA Purification kit (Invitrogen Corporation, Carlsbad, CA, USA) and one-tenth of the RNA was saved as the input control. Pierce[™] Protein A/G Magnetic Beads (Thermo Fisher Scientific, Waltham, MA, USA) were prewashed and incubated with 5 µg of anti-m⁶A antibody or rabbit IgG for 2 h at 4 °C with rotation. After 3 washes, the antibody-conjugated beads were mixed with purified poly (A) RNA, and 1 × immunoprecipitation buffer supplemented with RNase inhibitors. Then, the methylated mRNAs were precipitated with 5 mg of glycogen and one-tenth volume of 3 M sodium acetate in a 2.5 volume of 100% ethanol at -80 °C overnight after proteinase K digestion. Further enrichment was calculated by qPCR along with the MeRIP RNAs using primers listed in Table S9. The relative enrichment of m⁶A in each sample was calculated by normalizing the Cq value of the m⁶A-IP portion to the corresponding input portion.

Statistical analysis

All data (unless stated otherwise) are expressed as mean ± standard error of mean (SEM) and analyzed using GraphPad Prism software (v7.0). The comparisons of the Fs and Fts were made using the paired-samples design. For the results of RT-qPCR and WB, the statistical significance was calculated by using a paired *t*-test. Experiments were run in at least three independent replicates and differences were considered significant when $P < 0.05$.

Abbreviations

PPP1R3B: Protein phosphatase 1 regulatory subunit 3B; NADK2: NAD kinase 2, mitochondrial; HIF1A: Hypoxia inducible factor 1 subunit alpha; MYD88: MYD88 innate immune signal transduction adaptor; SLC9A3R1: SLC9A3 regulator 1; FOXO3: Forkhead box O3; MCUR1: Mitochondrial calcium uniporter regulator 1; FASN: Fatty acid synthase; PKM: Pyruvate kinase, muscle; AMPK: Adenosine monophosphate-activated protein kinase; mTOR: Mammalian target of rapamycin; MAPK: Mitogen-activated protein kinases

Supplementary Information

The online version contains supplementary material available at <https://doi.org/10.1186/s12864-021-07904-8>.

Additional file 1: Table S1. Sequencing data for fresh and frozen-thawed boar sperm

Additional file 2: Table S2-1. Methylated RNA sites on mRNAs in fresh and frozen-thawed sperm.

Additional file 3: Table S2-2. Differentially methylated sites on mRNAs

Additional file 4: Table S3. Genes containing the top ten hyper-methylated peaks in boar Fts compared with Fs

Additional file 5: Table S4. Genes containing the top ten hypo-methylated peaks in boar Fts compared with Fs

Additional file 6: Table S5-1. GO analysis of up-methylated mRNAs

Additional file 7: Table S5-2. GO analysis of down-methylated mRNAs

Additional file 8: Table S6-1. KEGG analysis of up-methylated mRNAs

Additional file 9: Table S6-2. KEGG analysis of down-methylated mRNAs

Additional file 10: Table S7-1. mRNA expression profile of fresh and frozen-thawed sperm

Additional file 11: Table S7-2. Differentially expressed mRNAs in fresh and frozen-thawed sperm

Additional file 12: Table S8. Joint analysis of differentially methylated sites and differentially expressed mRNAs

Additional file 13: Table S9. Primers used for RT-qPCR

Acknowledgements

We offer special thanks to Pengzhou Jinzhu Agricultural Development Co., Ltd for providing boar semen and the Cloudseq Biotech, Inc. (Shanghai, China) for the m⁶A MeRIP sequencing service and bioinformatics support. Moreover, we thank Dr Lin Zeng (BioDataStudio in Shanghai) for sequencing data analysis.

Authors' contributions

ZYQ, WCW, MAA, YZ and YHW collected samples, performed the experiments, analyzed the data and drafted the manuscript. MZ and JDY contributed to sample collection and data analysis and revised the manuscript. GBZ revised the manuscript critically and gave final approval for submission. CJZ granted, conceptualized the study, designed the experiments, revised the manuscript, and gave final approval of the manuscript. All authors reviewed and approved the final manuscript.

Funding

This research was supported by National Natural Science Foundation of China (NO: 31872356 and NO: 31570533). The funding bodies do not have any role in the design of the study, the collection, analysis and interpretation of data and the authoring of the manuscript.

Availability of data and materials

All raw transcriptome data reported in this article have been deposited to the NCBI's Gene Expression Omnibus, the web link is <https://www.ncbi.nlm.nih.gov/geo/query/acc.cgi?acc=GSE164691>.

Declarations

Ethics approval and consent to participate

All procedures for boar semen collection were reviewed and written approved by the Regulations for the Administration of Affairs Concerning Experimental Animals (Ministry of Science and Technology, China, revised in June 2004) and the Institutional Animal Care and Use Committee in the College of Animal Science and Technology, Sichuan Agricultural University, Sichuan, China, under permit No. DKYB20081003. The informed consent of the Pengzhou Jinzhu Agricultural Development Co., Ltd was obtained in verbal form to collect the boar semen for the purposes of this study.

Consent for publication

Not applicable.

Competing interests

The authors declare that they have no competing interests.

Author details

¹College of Animal Sciences and Technology, Sichuan Agricultural University, 611130 Chengdu, Sichuan, China. ²Farm Animal Genetic Resources Exploration and Innovation Key Laboratory of Sichuan Province, Sichuan

Agricultural University, 611130 Chengdu, Sichuan Province, China.

³Department of Theriogenology, Riphah College of Veterinary Sciences, 54000 Lahore, Pakistan.

Received: 23 October 2020 Accepted: 21 July 2021

Published online: 03 August 2021

References

- Bailey JL, Blodeau JF, Cormier N. Semen cryopreservation in domestic animals: a damaging and capacitating phenomenon minireview. *J Androl*. 2000;21(1):1–7.
- Ozkavukcu S, Erdemli E, Isik A, Oztuna D, Karahuseyinoglu S. Effects of cryopreservation on sperm parameters and ultrastructural morphology of human spermatozoa. *J Assist Reprod Genet*. 2008;25(8):403–11.
- Zhu ZD, Li RN, Lv YH, Zheng Y, Hoque SAM, Wu D, et al. Resveratrol improves boar sperm quality via 5'AMP-activated protein kinase activation during cryopreservation. *Oxid Med Cell Longev*. 2019;2019:5921503.
- Martin G, Sabido O, Durand P, Levy R. Cryopreservation induces an apoptosis-like mechanism in bull sperm. *Biol Reprod*. 2004;71(1):28–37.
- Khalifa T, Rekkas C, Samartzi F, Lymberopoulos A, Kousenidis K, Dovenski T. Highlights on artificial insemination (AI) technology in the pig. *Mac Vet Rev*. 2014;37(1):1–30.
- Carvajal G, Cuello C, Ruiz M, Vázquez JM, Martínez EA, Roca J. Effects of centrifugation before freezing on boar sperm cryosurvival. *J Androl*. 2004; 25(3):389–96.
- Knox RV. The fertility of frozen boar sperm when used for artificial insemination. *Reprod Domest Anim*. 2015;50(Suppl 2):90–7.
- Schagdarsurengin U, Steger K. Epigenetics in male reproduction: effect of paternal diet on sperm quality and offspring health. *Nat Rev Urol*. 2016; 13(10):584–95.
- Marcho C, Oluwayose OA, Pilsner JR. The preconception environment and sperm epigenetics. *Andrology*. 2020;8(4):924–42.
- Zeng CJ, Peng WP, Ding L, He L, Zhang Y, Fang DH, et al. A preliminary study on epigenetic changes during boar spermatozoa cryopreservation. *Cryobiology*. 2014;69(1):19–27.
- Aurich C, Schreiner B, Ille N, Alvarenga M, Scarlet D. Cytosine methylation of sperm DNA in horse semen after cryopreservation. *Theriogenology*. 2016; 86(5):1347–52.
- Machnicka MA, Olchowik A, Grosjean H, Bujnicki JM. Distribution and frequencies of post-transcriptional modifications in tRNAs. *RNA Biol*. 2014; 11(12):1619–29.
- Machnicka MA, Milanowska K, Osman Oglou O, Purta E, Kurkowska M, Olchowik A, et al. MODOMICS: a database of RNA modification pathways—2013 update. *Nucleic Acids Res*. 2013;41:D262–7.
- Meyer KD, Saletore Y, Zumbo P, Elemento O, Mason CE, Jaffrey SR. Comprehensive analysis of mRNA methylation reveals enrichment in 3' UTRs and near stop codons. *Cell*. 2012;149(7):1635–46.
- Wei CM, Moss B. Nucleotide sequences at the N⁶-methyladenosine sites of HeLa cell messenger ribonucleic acid. *Biochemistry*. 1977;16(8):1672–6.
- Wang ZG, Tang K, Zhang DY, Wan YZ, Wen Y, Lu QY, et al. High-throughput m⁶A-seq reveals RNA m⁶A methylation patterns in the chloroplast and mitochondria transcriptomes of Arabidopsis thaliana. *PLoS One*. 2017;12(11): e0185612.
- Levis R, Penman S. 5'-terminal structures of poly(A) + cytoplasmic messenger RNA and of poly(A) + and poly(A)- heterogeneous nuclear RNA of cells of the dipteran *Drosophila melanogaster*. *J Mol Biol*. 1978;120(4): 487–515.
- Clancy MJ, Shambaugh ME, Timpte CS, Bokar JA. Induction of sporulation in *Saccharomyces cerevisiae* leads to the formation of N⁶-methyladenosine in mRNA: a potential mechanism for the activity of the IME4 gene. *Nucleic Acids Res*. 2002;30(20):4509–18.
- Manners O, Baquero-Perez B, Whitehouse A. m⁶A: Widespread regulatory control in virus replication. *Biochim Biophys Acta Gene Regul Mech*. 2019; 1862(3):370–81.
- Fu Y, Dominissini D, Rechavi G, He C. Gene expression regulation mediated through reversible m⁶A RNA methylation. *Nat Rev Genet*. 2014;15(5):293–306.
- Edupuganti RR, Geiger S, Lindeboom RGH, Shi H, Hsu PJ, Lu Z, et al. N⁶-methyladenosine (m⁶A) recruits and repels proteins to regulate mRNA homeostasis. *Nat Struct Mol Biol*. 2017;24(10):870–8.

22. Wang X, Zhao BS, Roundtree IA, Lu Z, Han D, Ma H, et al. N⁶-methyladenosine modulates messenger RNA translation efficiency. *Cell*. 2015;161(6):1388–99.
23. Louloui A, Ntini E, Conrad T, Orom UAV. Transient N⁶-Methyladenosine transcriptome sequencing reveals a regulatory role of m⁶A in splicing efficiency. *Cell Rep*. 2018;23(12):3429–37.
24. Lin Z, Hsu PJ, Xing XD, Fang JH, Lu ZK, Zou Q, et al. Mettl3-/Mettl14-mediated mRNA N⁶-methyladenosine modulates murine spermatogenesis. *Cell Res*. 2017;27(10):1216–30.
25. Zheng G, Dahl JA, Niu Y, Fedorcsak P, Huang CM, Li CJ, et al. ALKBH5 is a mammalian RNA demethylase that impacts RNA metabolism and mouse fertility. *Mol Cell*. 2013;49(1):18–29.
26. Tang C, Klukovich R, Peng HY, Wang ZQ, Yu T, Zhang Y, et al. ALKBH5-dependent m⁶A demethylation controls splicing and stability of long 3'-UTR mRNAs in male germ cells. *Proc Natl Acad Sci USA*. 2018;115(2):E325–33.
27. Tang C, Xie YM, Yu T, Liu N, Wang ZQ, Woolsey RJ, et al. m⁶A-dependent biogenesis of circular RNAs in male germ cells. *Cell Res*. 2020;30(3):211–28.
28. Yang Y, Huang W, Huang JT, Shen F, Xiong J, Yuan EF, et al. Increased N⁶-methyladenosine in human sperm RNA as a risk factor for asthenozoospermia. *Sci Rep*. 2016;6:24345.
29. Landfors M, Nakken S, Fusser M, Dahl JA, Klungland A, Fedorcsak P. Sequencing of FTO and ALKBH5 in men undergoing infertility work-up identifies an infertility-associated variant and two missense mutations. *Fertil Steril*. 2016;105(5):1170–9.e1175.
30. Godia M, Mayer FQ, Nafissi J, Castelló A, Rodríguez-Gil JE, Sánchez A, et al. A technical assessment of the porcine ejaculated spermatozoa for a sperm-specific RNA-seq analysis. *Syst Biol Reprod Med*. 2018;64(4):291–303.
31. Fraser L, Brym P, Pareek CS, Mogielnicka-Brzozowska M, Pauksztó Ł, Jastrzebski JP, et al. Transcriptome analysis of boar spermatozoa with different freezability using RNA-Seq. *Theriogenology*. 2020;142:400–13.
32. He YQ, Maltecca C, Tiezzi F, Soto EL, Flowers WL. Transcriptome analysis identifies genes and co-expression networks underlying heat tolerance in pigs. *BMC Genet*. 2020;21(1):44.
33. McIntyre ABR, Gokhale NS, Cerchietti L, Jaffrey SR, Horner SM, Mason CE. Limits in the detection of m⁶A changes using MeRIP/m⁶A-seq. *Sci Rep*. 2020;10(1):6590.
34. Zhu W, Cheng X, Ren CH, Chen JH, Zhang Y, Chen YL, et al. Proteomic characterization and comparison of ram (*Ovis aries*) and buck (*Capra hircus*) spermatozoa proteome using a data independent acquisition mass spectrometry (DIA-MS) approach. *PLoS One*. 2020;15(2):e0228656.
35. Pini T, Leahy T, Soleilhavoup C, Tsikis G, Labas V, Combes-Soia L, et al. Proteomic investigation of ram spermatozoa and the proteins conferred by seminal plasma. *J Proteome Res*. 2016;15(10):3700–11.
36. Bajpai M, Fiedler SE, Huang Z, Vijayaraghavan S, Olson GE, Livera G, et al. AKAP3 selectively binds PDE4A isoforms in bovine spermatozoa. *Biol Reprod*. 2006;74(1):109–18.
37. Tan Y, Demeter MR, Ruan H, Comb MJ. BAD Ser-155 phosphorylation regulates BAD/Bcl-XL interaction and cell survival. *J Biol Chem*. 2000;275(33):25865–9.
38. Sun P, Zeng Q, Cheng DQ, Zhang K, Zheng JL, Liu YP, et al. Caspase recruitment domain protein 6 protects against hepatic steatosis and insulin resistance by suppressing apoptosis signal-regulating kinase 1. *Hepatology*. 2018;68(6):2212–29.
39. Etkovitz N, Rubinstein S, Daniel L, Breitbart H. Role of PI3-Kinase and PI4-Kinase in Actin Polymerization During Bovine Sperm Capacitation. *Biol Reprod*. 2007;77(2):263–73.
40. Jankowska A, Burczyńska B, Duda T, Warchol JB. Rod outer segment membrane guanylate cyclase type 1 (ROS-GC1) calcium-modulated transduction system in the sperm. *Fertil Steril*. 2010;93(3):904–12.
41. Alankarage D, Lavery R, Svingen T, Kelly S, Ludbrook L, Bagheri-Fam S, et al. SOX9 regulates expression of the male fertility gene Ets variant factor 5 (ETV5) during mammalian sex development. *Int J Biochem Cell Biol*. 2016; 79:41–51.
42. Choi D, Lee E, Hwang S, Jun K, Kim D, Yoon BK, et al. The biological significance of phospholipase C beta 1 gene mutation in mouse sperm in the acrosome reaction, fertilization, and embryo development. *J Assist Reprod Genet*. 2001;18(5):305–10.
43. Bilodeau JF, Chatterjee S, Sirard MA, Gagnon C. Levels of antioxidant defenses are decreased in bovine spermatozoa after a cycle of freezing and thawing. *Mol Reprod Dev*. 2000;55(3):282–8.
44. Bailey J, Morrier A, Cormier N. Semen cryopreservation: Successes and persistent problems in farm species. *Can J Anim Sci*. 2003;83(3):393–401.
45. Donnelly ET, McClure N, Lewis SEM. Cryopreservation of human semen and prepared sperm: effects on motility parameters and DNA integrity. *Fertil Steril*. 2001;76(5):892–900.
46. Saleh RA, Agarwal A. Oxidative stress and male infertility: from research bench to clinical practice. *J Androl*. 2002;23(6):737–52.
47. Nowicka-Bauer K, Nixon B. Molecular changes induced by oxidative stress that impair human sperm motility. *Antioxidants (Basel)*. 2020;9(2):134.
48. Peña FJ, Plaza Davila M, Ball BA, Squires EL, Martin Muñoz P, Ortega Ferrusola C, et al. The impact of reproductive technologies on stallion mitochondrial function. *Reprod Domest Anim*. 2015;50(4): 529–37.
49. Fraser L. Markers for sperm freezability and relevance of transcriptome studies in semen cryopreservation: a review. *Theriogenology*, Rita Payan Carreira, IntechOpen. 2017.
50. Yeste M. Sperm cryopreservation update: Cryodamage, markers, and factors affecting the sperm freezability in pigs. *Theriogenology*. 2016;85(1):47–64.
51. O'Connell M, McClure N, Lewis SEM. The effect of cryopreservation on sperm morphology, motility and mitochondrial function. *Hum Reprod*. 2002; 17(3):704–9.
52. Hezavehei M, Sharafi M, Kouchesfahani HM, Henkel R, Agarwal A, Esmaeili V, et al. Sperm cryopreservation: A review on current molecular cryobiology and advanced approaches. *Reprod Biomed Online*. 2018;37(3):327–39.
53. Zhao TX, Wang JK, Shen LJ, Long CL, Liu B, Wei Y, et al. Increased m⁶A RNA modification is related to the inhibition of the Nrf2-mediated antioxidant response in di-(2-ethylhexyl) phthalate-induced prepubertal testicular injury. *Environ Pollut*. 2020;259:113911.
54. Anders M, Chelysheva I, Goebel I, Trenkner T, Zhou J, Mao YH, et al. Dynamic m⁶A methylation facilitates mRNA triaging to stress granules. *Life Sci Alliance*. 2018;1(4):e201800113.
55. Yu R, Li Q, Feng Z, Cai L, Xu Q. m⁶A reader YTHDF2 regulates LPS-induced inflammatory response. *Int J Mol Sci*. 2019;20(6):1323.
56. Ren X, Chen X, Wang Z, Wang D. Is transcription in sperm stationary or dynamic? *J Reprod Dev*. 2017;63(5):439–43.
57. LyMBERG RA, Evans JP, Kennington WJ. Post-ejaculation thermal stress causes changes to the RNA profile of sperm in an external fertilizer. *Proc Biol Sci*. 1938;2020(287):20202147.
58. Zhao TH, Li XY, Sun DL, Zhang ZZ. Oxidative stress: One potential factor for arsenite-induced increase of N⁶-methyladenosine in human keratinocytes. *Environ Toxicol Pharmacol*. 2019;69:95–103.
59. He YC, Xing J, Wang SY, Xin SJ, Han YS, Zhang J. Increased m⁶A methylation level is associated with the progression of human abdominal aortic aneurysm. *Ann Transl Med*. 2019;7(24):797.
60. Tang B, Yang YH, Kang M, Wang YS, Wang Y, Bi Y, et al. m⁶A demethylase ALKBH5 inhibits pancreatic cancer tumorigenesis by decreasing WIF-1 RNA methylation and mediating Wnt signaling. *Mol Cancer*. 2020;19(1):3.
61. Li JF, Xie HY, Ying YF, Chen H, Yan HQ, He LJ, et al. YTHDF2 mediates the mRNA degradation of the tumor suppressors to induce AKT phosphorylation in N⁶-methyladenosine-dependent way in prostate cancer. *Mol Cancer*. 2020;19(1):152.
62. Zaccara S, Jaffrey SR. A unified model for the function of YTHDF proteins in regulating m⁶A-modified mRNA. *Cell*. 2020;181(7):1582–95.
63. Wei CM, Gershowitz A, Moss B. 5'-Terminal and internal methylated nucleotide sequences in HeLa cell mRNA. *Biochemistry*. 1976;15(2):397–401.
64. Luo GZ, MacQueen A, Zheng G, Duan H, Dore LC, Lu Z, et al. Unique features of the m⁶A methylome in *Arabidopsis thaliana*. *Nat Commun*. 2014; 5:5630.
65. Dominissini D, Moshitch-Moshkovitz S, Schwartz S, et al. Topology of the human and mouse m⁶A RNA methylomes revealed by m⁶A-seq. *Nature*. 2012;485(7397):201–6.
66. Tao XL, Chen JN, Jiang YZ, Wei YY, Chen Y, Xu HM, et al. Transcriptome-wide N⁶-methyladenosine methylome profiling of porcine muscle and adipose tissues reveals a potential mechanism for transcriptional regulation and differential methylation pattern. *BMC Genom*. 2017;18(1):336.
67. Niu X, Xu J, Liu J, Chen L, Qiao X, Zhong M. Landscape of N⁶-methyladenosine modification patterns in human Ameloblastoma. *Front Oncol*. 2020;10:556497.
68. Cheng BH, Leng L, Li ZW, Wang WJ, Jing Y, Li YD, et al. Profiling of RNA N⁶-Methyladenosine methylation reveals the critical role of m⁶A in Chicken adipose deposition. *Front Cell Dev Biol*. 2021;9:590468.

69. Wang YJ, Zeng L, Liang C, Zan R, Ji WP, Zhang ZC, et al. Integrated analysis of transcriptome-wide m6A methylome of osteosarcoma stem cells enriched by chemotherapy. *Epigenomics*. 2019;11(15):1693–715.
70. Martin-Cano FE, Gaitskell-Phillips G, Ortiz-Rodriguez JM, Silva-Rodriguez A, Roman A, Rojo-Dominguez P, et al. Proteomic profiling of stallion spermatozoa suggests changes in sperm metabolism and compromised redox regulation after cryopreservation. *J Proteomics*. 2020;221:103765.
71. Zhong DD, Chen MJ, Zhang L, Chen H, Shi DS, Liu QY, et al. Aberrant regulation of RNA methylation during spermatogenesis. *Reprod Domest Anim*. 2020;56(1):3–11.
72. Sadler-Riggelman I, Klukovich R, Nilsson E, Beck D, Xie Y, Yan W, et al. Epigenetic transgenerational inheritance of testis pathology and Sertoli cell epimutations: generational origins of male infertility. *Environ Epigenet*. 2019; 5(3):dvz013.
73. Xie XM, Deng T, Duan JF, Xie J, Yuan JL, Chen MQ. Exposure to polystyrene microplastics causes reproductive toxicity through oxidative stress and activation of the p38 MAPK signaling pathway. *Ecotoxicol Environ Saf*. 2020; 190:110133.
74. Silva JV, Cabral M, Correia BR, Carvalho P, Sousa M, Oliveira PF, et al. mTOR signaling pathway regulates sperm quality in older men. *Cells*. 2019;8(6):629.
75. Petelak A, Krylov V. Surface sperm cell ubiquitination directly impaired blastocyst formation rate after intracytoplasmic sperm injection in pig. *Theriogenology*. 2019;135:115–20.
76. Purdy PH. Ubiquitination and its influence in boar sperm physiology and cryopreservation. *Theriogenology*. 2008;70(5):818–26.
77. Deng CY, Lv M, Luo BH, Zhao SZ, Mo ZC, Xie YJ. The role of the PI3K/AKT/mTOR signalling pathway in male reproduction. *Curr Mol Med*. 2020;21(7): 539–48.
78. Karabulut S, Demiroğlu-Zergeroğlu A, Yılmaz E, Sağır F, Delikara N. p53 and mitogen-activated protein kinase pathway protein profiles in fresh and frozen spermatozoa. *Andrologia*. 2014;46(10):1113–7.
79. Sun ZL, Zhang W, Li SJ, Xue XC, Niu RY, Shi L, et al. Altered miRNAs expression profiling in sperm of mice induced by fluoride. *Chemosphere*. 2016;155:109–14.
80. Alves-Fernandes DK, Jasiulionis MG. The role of SIRT1 on DNA damage response and epigenetic alterations in cancer. *Int J Mol Sci*. 2019;20(13):3153.
81. Mostafa T, Nabil N, Rashed L, Abo-Sief AF, Eissa HH. Seminal SIRT1-oxidative stress relationship in infertile oligoasthenoteratozoospermic men with varicocele after its surgical repair. *Andrologia*. 2020;52(1):e13456.
82. Coussens M, Maresh JG, Yanagimachi R, Maeda G, Allsopp R. Sirt1 deficiency attenuates spermatogenesis and germ cell function. *PLoS One*. 2008;3(2): e1571.
83. Islam S, Uehara O, Matsuoka H, Kuramitsu Y, Adhikari BR, Hiraki D, et al. DNA hypermethylation of sirtuin 1 (SIRT1) caused by betel quid chewing—a possible predictive biomarker for malignant transformation. *Clin Epigenetics*. 2020;12(1):12.
84. Li B, He X, Zhuang MR, Niu BW, Wu CY, Mu HL, et al. Melatonin ameliorates busulfan-induced spermatogonial stem cell oxidative apoptosis in mouse testes. *Antioxid Redox Signal*. 2018;28(5):385–400.
85. An CN, Jiang H, Wang Q, Yuan RP, Liu JM, Shi WL, et al. Down-regulation of DJ-1 protein in the ejaculated spermatozoa from Chinese asthenozoospermia patients. *Fertil Steril*. 2011;96(1):19–23.e12.
86. Ooe H, Taira T, Iguchi-Aruga SM, Ariga H. Induction of reactive oxygen species by bisphenol A and abrogation of bisphenol A-induced cell injury by DJ-1. *Toxicol Sci*. 2005;88(1):114–26.
87. Sun Y, Zhang WJ, Zhao X, Yuan RP, Jiang H, Pu XP. PARK7 protein translocating into spermatozoa mitochondria in Chinese asthenozoospermia. *Reproduction*. 2014;148(3):249–57.
88. Heidary Z, Zaki-Dizaji M, Saliminejad K, Edalatkhah H, Khorram Khorshid HR. MiR-4485-3p expression reduced in spermatozoa of men with idiopathic asthenozoospermia. *Andrologia*. 2020;52(3):e13539.
89. Zou JX, Duan Z, Wang J, Sokolov A, Xu J, Chen CZ, et al. Kinesin family deregulation coordinated by bromodomain protein ANCCA and histone methyltransferase MLL for breast cancer cell growth, survival, and tamoxifen resistance. *Mol Cancer Res*. 2014;12(4):539–49.
90. Wu ZQ, Zhang H, Sun ZW, Wang CM, Chen Y, Luo P, et al. Knockdown of kinesin family 15 inhibits osteosarcoma through suppressing cell proliferation and promoting cell apoptosis. *Chemotherapy*. 2019;64(4):187–96.
91. Gordon MA, Babbs B, Cochrane DR, Bitler BG, Richer JK. The long non-coding RNA MALAT1 promotes ovarian cancer progression by regulating RBFOX2-mediated alternative splicing. *Mol Carcinog*. 2018;58(2):196–205.
92. Shen J, Zhang JH, Xiao H, Wu JM, He KM, Lv ZZ, et al. Mitochondria are transported along microtubules in membrane nanotubes to rescue distressed cardiomyocytes from apoptosis. *Cell Death Dis*. 2018;9(2):81.
93. Panner Selvam MK, Agarwal A, Pushparaj PN. Altered molecular pathways in the proteome of cryopreserved sperm in testicular cancer patients before treatment. *Int J Mol Sci*. 2019;20(3):677.
94. Agarwal A, Panner Selvam MK, Samanta L, Vij SC, Parekh N, Sabaneh E, et al. Effect of antioxidant supplementation on the sperm proteome of idiopathic infertile men. *Antioxidants (Basel)*. 2019;8(10):488.
95. Cao WL, Aghajanian HK, Haig-Ladewig LA, Gerton GL. Sorbitol can fuel mouse sperm motility and protein tyrosine phosphorylation via sorbitol dehydrogenase. *Biol Reprod*. 2009;80(1):124–33.
96. Dai JB, Xu WJ, Zhao XL, Zhang MX, Zhang D, Nie DS, et al. Protein profile screening: reduced expression of Sord in the mouse epididymis induced by nicotine inhibits tyrosine phosphorylation level in capacitated spermatozoa. *Reproduction*. 2016;151(3):227–37.
97. Asghari A, Marashi SA, Ansari-Pour N. A sperm-specific proteome-scale metabolic network model identifies non-glycolytic genes for energy deficiency in asthenozoospermia. *Syst Biol Reprod Med*. 2017;63(2):100–12.
98. Dai DH, Qazi I, Ran MX, Liang K, Zhang Y, Zhang M, et al. Exploration of miRNA and mRNA profiles in fresh and frozen-thawed boar sperm by transcriptome and small RNA sequencing. *Int J Mol Sci*. 2019;20(4):802.
99. Agarwal A, Sharma R, Durairajanayagam D, Ayaz A, Cui Z, Willard B, et al. Major protein alterations in spermatozoa from infertile men with unilateral varicocele. *Reprod Biol Endocrinol*. 2015;13:8.
100. Cherry JA, Pho V. Characterization of cAMP degradation by phosphodiesterases in the accessory olfactory system. *Chem Senses*. 2002; 27(7):643–52.
101. Spehr M, Gisselmann G, Poplawski A, Riffell JA, Wetzel CH, Zimmer RK, et al. Identification of a testicular odorant receptor mediating human sperm chemotaxis. *Science*. 2003;299(5615):2054–8.
102. Chandrani A, Sofia W, Christer L. Down regulation of CLDN1 induces apoptosis in breast cancer cells. *PLoS One*. 2015;10(6):e0130300.
103. Akichika S, Hirano S, Shichino Y, Suzuki T, Nishimasu H, Ishitani R, et al. Cap-specific terminal N⁶-methylation of RNA by an RNA polymerase II-associated methyltransferase. *Science*. 2018;363(6423):eaav0080.
104. Huang HL, Weng HY, Zhou KR, Wu T, Zhao BS, Sun ML, et al. Histone H3 trimethylation at lysine 36 guides m⁶A RNA modification co-transcriptionally. *Nature*. 2019;567(7748):414–9.
105. Liu J, Dou XY, Chen CY, Chen C, Liu C, Xu MM, et al. N⁶-methyladenosine of chromosome-associated regulatory RNA regulates chromatin state and transcription. *Science*. 2020;367(6477):580–6.
106. Guo HM, Wang B, Xu KY, Nie L, Fu Y, Wang ZD, et al. m⁶A reader HNRN PA2B1 promotes esophageal cancer progression via up-regulation of ACLY and ACC1. *Front Oncol*. 2020;10:553045.
107. Sun DL, Zhao TH, Zhang Q, Wu M, Zhang ZZ. Fat mass and obesity-associated protein regulates lipogenesis via m⁶A modification in fatty acid synthase mRNA. *Cell Biol Int*. 2020;45(2):334–44.
108. Zeng CJ, Tang KY, He L, Peng WP, Ding L, Fang DH, et al. Effects of glycerol on apoptotic signaling pathways during boar spermatozoa cryopreservation. *Cryobiology*. 2014;68(3):395–404.
109. Wang WC, Liang K, Chang Y, Ran MX, Zhang Y, Ali MA, et al. miR-26a is involved in glycometabolism and affects boar sperm viability by targeting PDHX. *Cells*. 2020;9(1):146.
110. Livak KJ, Schmittgen TD. Analysis of relative gene expression data using real-time quantitative PCR and the 2⁻(Delta Delta C(T)) Method. *Methods*. 2001;25(4):402–8.
111. Zeng CJ, He L, Peng WP, Ding L, Tang KY, Fang DH, et al. Selection of optimal reference genes for quantitative RT-PCR studies of boar spermatozoa cryopreservation. *Cryobiology*. 2014;68(1):113–21.
112. Martin M. Cutadapt removes adapter sequences from high-throughput sequencing reads. *EMBnet J*. 2011;17(1):10–2.
113. Kim D, Langmead B, Salzberg S. HISAT: a fast spliced aligner with low memory requirements. *Nat Methods*. 2015;12(4):357–60.
114. Zhang Y, Liu T, Meyer CA, Eeckhoutte J, Johnson DS, Bernstein BE, et al. Model-based analysis of ChIP-Seq (MACS). *Genome Biol*. 2008;9(9):R137.
115. Shen L, Shao NY, Liu XC, Maze I, Feng J, Nestler EJ, et al. diffReps: Detecting Differential Chromatin Modification Sites from ChIP-seq Data with Biological Replicates. *PLoS One*. 2013;8(6):e65598.
116. Bailey TL. STREME: Accurate and versatile sequence motif discovery. *Bioinformatics*. 2020;btab203.

117. Simon A, Theodor PP, Wolfgang H. HTSeq—a Python framework to work with high-throughput sequencing data. *Bioinformatics*. 2014;31(2):166–9.
118. Robinson MD, Mccarthy DJ, Smyth GK. edgeR: a Bioconductor package for differential expression analysis of digital gene expression data. *Bioinformatics*. 2010;26(1):139–40.

Publisher's Note

Springer Nature remains neutral with regard to jurisdictional claims in published maps and institutional affiliations.

Ready to submit your research? Choose BMC and benefit from:

- fast, convenient online submission
- thorough peer review by experienced researchers in your field
- rapid publication on acceptance
- support for research data, including large and complex data types
- gold Open Access which fosters wider collaboration and increased citations
- maximum visibility for your research: over 100M website views per year

At BMC, research is always in progress.

Learn more biomedcentral.com/submissions

